

# Phase retrieval using spatially modulated illumination

Peng Gao,<sup>1,2,\*</sup> Giancarlo Pedrini,<sup>1</sup> Chao Zuo,<sup>1,3</sup> and Wolfgang Osten<sup>1</sup>

<sup>1</sup>Institut für Technische Optik, Universität Stuttgart, Pfaffenwaldring 9, 70569 Stuttgart, Germany

<sup>2</sup>State Key Laboratory of Transient Optics and Photonics, Xi'an Institute of Optics and Precision Mechanics, Chinese Academy of Sciences, Xi'an 710119, China

<sup>3</sup>Centre for Optical and Laser Engineering, School of Mechanical and Aerospace Engineering, Nanyang Technological University, Singapore

\*Corresponding author: peng.gao@ito.uni-stuttgart.de

Received March 31, 2014; revised May 14, 2014; accepted May 15, 2014;  
posted May 15, 2014 (Doc. ID 209291); published June 11, 2014

In this Letter, we propose a method for retrieving the phase of a wavefront from the diffraction patterns recorded when the object is sequentially illuminated by spatially modulated light. For wavefronts having a smooth phase, the retrieval is achieved by using a deterministic method. When the phase has discontinuities, an iterative process is used for the retrieval and enhancement of the spatial resolution. Both the deterministic and iterative phase reconstructions are demonstrated by experiments. © 2014 Optical Society of America

OCIS codes: (180.0180) Microscopy; (110.1650) Coherence imaging.  
<http://dx.doi.org/10.1364/OL.39.003615>

Phase imaging is of fundamental importance for technical and biomedical investigations, since the phase contains information about the 3D shape and the inner structure of transparent or translucent samples. Holography is the most commonly used approach to retrieve the phase, where an additional reference wave is superimposed on the object wave and the phase is reconstructed from the generated interference pattern [1–4]. This approach has high accuracy, but the use of an independent reference wave makes it sensitive to external perturbations, such as vibrations and temperature changes, and leads to an increase in the setup complexity. Methods based on a Shack–Hartmann sensor [5], pyramid sensor [6], hologram-based sensor [7], or shearing interferometers [8] are used for the phase investigation of smooth wavefronts. Furthermore, the beam-propagation-based methods [9–16] estimate the phase by iterative propagating of the wave among a sequence of diffraction patterns. The diffraction patterns may be recorded at different axial planes [9,10], with different wavelengths [11], by flipping the sample [12], by modulating the object wave with different phase patterns [13,14], or by scanning an aperture over the object wave [15–17]. There are, as well, deterministic methods retrieving the phase by using the transport of intensity equation (TIE) [18–25]. The TIE method records two or three diffraction patterns at closely spaced planes and reconstructs the phase without the iteration process.

In this Letter, we propose a phase retrieval method by using time-sequential spatially modulated illuminations. For wavefronts with a smooth phase, a deterministic phase retrieval is performed by solving the phase gradient instead of the phase second derivative (Laplacian). An iterative process is used to reconstruct the phase of wavefronts having discontinuities and at the same time enhance the spatial resolution. Unlike the traditional TIE, which records the object wave intensities in two or more axially spaced planes, this method records the intensity patterns in a single plane.

Figure 1 shows the setup used for the phase retrieval, where a collimated beam is modulated by a spatial light modulator (SLM) and imaged to the sample by a

telescopic system composed of the lenses  $L_1$  and  $L_2$ . Another telescopic system composed of the lenses  $L_3$  and  $L_4$  reconstructs an inverted and magnified image of the sample in the image plane (IM) located at the axial distance  $dz$  from the CCD sensor. We will use a sequence of illuminations, and their complex amplitudes in the sample plane are denoted with  $A_m^{\text{illum}}$ ; for  $m = 0$ ,  $A_0^{\text{illum}}$  is a plane wave with constant intensity and phase, and for  $m = 1, 2, \dots, M$ ,  $A_m^{\text{illum}}$  are the spatially modulated waves. When the sample is inserted and illuminated by the waves  $A_m^{\text{illum}}$ , the complex amplitude in the IM is  $A_m^{\text{IM}} = \sqrt{I_m^{\text{IM}}} \exp\{i\varphi_m^{\text{IM}}\}$ . The intensities of the object waves recorded by the CCD are denoted as  $I_m^{\text{CCD}}$ . According to the TIE [18–25], the phase  $\varphi_m^{\text{IM}}$  of the object wave under the  $m$ th illumination is related to the two intensities  $I_m^{\text{IM}}$  and  $I_m^{\text{CCD}}$  as follows:

$$\nabla \cdot [I_m^{\text{IM}} \nabla \varphi_m^{\text{IM}}] = -\frac{2\pi}{\lambda} \cdot \frac{I_m^{\text{CCD}} - I_m^{\text{IM}}}{dz}, \quad (1)$$

where  $\nabla = \nabla_x \vec{e}_x + \nabla_y \vec{e}_y$  is the 2D gradient operator in the  $xy$  plane and  $\vec{e}_x, \vec{e}_y$  are unit directional vectors. It is preferable to choose a small  $dz$  in order to have a good approximation when we replace  $\partial I / \partial z$  with  $(I_m^{\text{CCD}} - I_m^{\text{IM}}) / dz$  in Eq. (1).  $A_0^{\text{IM}}$  describes the transmission of the sample when illuminated by the plane wave  $A_0^{\text{illum}}$ , and thus for the modulated illumination  $A_m^{\text{illum}}$ , which has the complex amplitude  $A_m^{\text{illum,IM}}$  at the IM, we have  $A_m^{\text{IM}} = A_m^{\text{illum,IM}} \cdot A_0^{\text{IM}}$ , i.e.,  $I_m^{\text{IM}} = I_m^{\text{illum,IM}} I_0^{\text{IM}}$ ,  $\varphi_m^{\text{IM}} = \varphi_m^{\text{illum,IM}} + \varphi_0^{\text{IM}}$ .

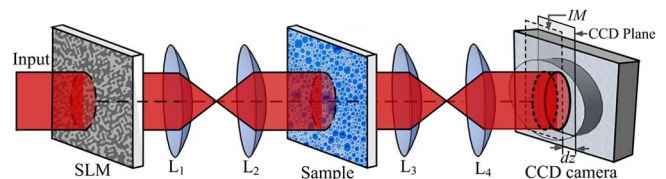


Fig. 1. Setup of the phase retrieval by using spatially modulated illuminations. SLM, spatial light modulator;  $L_1$ – $L_4$ , achromatic lenses; IM, image plane;  $dz$ , the distance between imaging plane and CCD plane.

$I_m^{\text{illum,IM}}$  and  $\varphi_m^{\text{illum,IM}}$  denote the intensity and phase of the  $m$ th illumination in the IM, for the case where no sample is inserted in the system. By considering the TIEs for plane wave  $\nabla \cdot [I_0^{\text{IM}} \nabla \varphi_0^{\text{IM}}] = -2\pi(I_0^{\text{CCD}} - I_0^{\text{IM}})/(\lambda dz)$ , for modulated illuminations  $\nabla \cdot [I_m^{\text{IM}} \nabla \varphi_0^{\text{IM}}] = -2\pi(I_m^{\text{CCD}} - I_m^{\text{IM}})/(\lambda dz)$ , and for relations  $I_m^{\text{IM}} = I_m^{\text{illum,IM}} I_0^{\text{IM}}$ ,  $\varphi_m^{\text{IM}} = \varphi_m^{\text{illum,IM}} + \varphi_0^{\text{IM}}$ , we obtain

$$c_{m,1} I_0^{\text{IM}} + c_{m,2} \partial_x I_0^{\text{IM}} + c_{m,3} \partial_y I_0^{\text{IM}} + c_{m,4} I_0^{\text{IM}} \partial_x \varphi_0^{\text{IM}} + c_{m,5} I_0^{\text{IM}} \partial_y \varphi_0^{\text{IM}} = d_m. \quad (2)$$

$\partial_x$  and  $\partial_y$  denote the partial derivatives in the  $x$  and  $y$  directions, and the coefficients  $c_{m,1}$ ,  $c_{m,2}$ ,  $c_{m,3}$ ,  $c_{m,4}$ ,  $c_{m,5}$  are

$$\begin{aligned} c_{m,1} &= I_m^{\text{illum,IM}} \Delta \varphi_m^{\text{illum,IM}} + \nabla I_m^{\text{illum,IM}} \cdot \nabla \varphi_m^{\text{illum,IM}}, \\ c_{m,2} &= I_m^{\text{illum,IM}} \partial_x \varphi_m^{\text{illum,IM}}, \\ c_{m,3} &= I_m^{\text{illum,IM}} \partial_y \varphi_m^{\text{illum,IM}}, \\ c_{m,4} &= \partial_x I_m^{\text{illum,IM}}, \\ c_{m,5} &= \partial_y I_m^{\text{illum,IM}}, \\ d_m &= -\frac{2\pi}{\lambda_0} \cdot \frac{I_m^{\text{CCD}} - I_0^{\text{CCD}} I_m^{\text{illum,IM}}}{dz}. \end{aligned} \quad (3)$$

At least five equations are needed to calculate  $I_0^{\text{IM}}$ ,  $\partial_x \varphi_0^{\text{IM}}$ , and  $\partial_y \varphi_0^{\text{IM}}$  from Eq. (2), and thus we need to record intensity patterns when the sample is illuminated by a plane wave and at least five spatially modulated waves. We may write the five linear equations as follows:

$$\begin{bmatrix} c_{11} & c_{12} & c_{13} & c_{14} & c_{15} \\ c_{21} & c_{22} & c_{23} & c_{24} & c_{25} \\ c_{31} & c_{32} & c_{33} & c_{34} & c_{35} \\ c_{41} & c_{42} & c_{43} & c_{44} & c_{45} \\ c_{51} & c_{52} & c_{53} & c_{54} & c_{55} \end{bmatrix} \begin{bmatrix} I_0^{\text{IM}} \\ \partial_x I_0^{\text{IM}} \\ \partial_y I_0^{\text{IM}} \\ I_0 \partial_x \varphi_0^{\text{IM}} \\ I_0 \partial_y \varphi_0^{\text{IM}} \end{bmatrix} = \begin{bmatrix} d_1 \\ d_2 \\ d_3 \\ d_4 \\ d_5 \end{bmatrix}. \quad (4)$$

The coefficients  $c_{m,n}$  in Eq. (4) are related to the intensity and phase distributions of the illumination waves. The amplitude and phase of the illumination waves need to be known, and in practice this can be achieved by generating the illuminations with a SLM, which is calibrated to have a known relation between the pixels' gray value and the phase [4]. It should be considered as well that the illumination is low pass filtered by the telescopic system  $L_1$ – $L_2$ . The complex amplitudes of the illumination waves can be optimized such that the absolute values of the five eigenvalues of the coefficient matrix in Eq. (4) have approximately the same magnitude, i.e., the condition number of the coefficient matrix is minimized [26,27]. In this case, according to the perturbation theory of linear algebraic systems, the solution of Eq. (4) is less sensitive to the measurement uncertainty of the intensities. A more robust reconstruction with noise reduction can be realized by using more illuminations in order to built an  $M \times 5$  matrix  $C_{M \times 5}$  ( $M > 5$ ). Instead of Eq. (4), we will have  $C_{M \times 5} \cdot X = D_M$ , where  $X = [I_0^{\text{IM}}, \partial_x I_0^{\text{IM}}, \partial_y I_0^{\text{IM}}, \partial_x \varphi_0^{\text{IM}}, \partial_y \varphi_0^{\text{IM}}]^T$  and  $D_M = [d_1, d_2, \dots, d_M]^T$ . The overdetermined linear equation

system is solved by using the least-square method, where the two sides of the linear equation system are multiplied with the transposed matrix  $C_{M \times 5}^T$  and  $X = [C_{M \times 5}^T C_{M \times 5}]^{-1} C_{M \times 5}^T D_M$ . It is possible to use illuminations with periodic distributions, e.g.,  $A_m^{\text{illum}} = A_0 \cos(\vec{\kappa}_m \cdot \vec{r})$  or  $A_m^{\text{illum}} = A_0 \exp[i2\pi \cos(\vec{\kappa}_m \cdot \vec{r})]$ . Here,  $A_0$  is a constant and  $\vec{r}$  is the position vector. In this case, for the phase retrieval we only need to know the wave vector  $\vec{\kappa}_m$  for each illumination. Furthermore, these two kinds of illuminations can also simplify the solution of Eq. (4).

The retrieval of the phase can be done by using only three illuminations (one plane and two spatially modulated), when the following approximation is used:

$$I_0^{\text{IM}} = I_0^{\text{CCD}} + \frac{\lambda dz}{2\pi} [\nabla I_0^{\text{CCD}} \cdot \nabla \varphi_0^{\text{IM}} + I_0^{\text{CCD}} \Delta \varphi_0^{\text{IM}}]. \quad (5)$$

This equation is derived directly from the TIE for the plane wave illumination, and by replacing  $I_0^{\text{IM}}$  with  $I_0^{\text{CCD}}$  in the bracket. By inserting Eq. (5) into Eq. (2), we obtain

$$\begin{bmatrix} a_{1,1} & a_{1,2} \\ a_{2,1} & a_{2,2} \end{bmatrix} \begin{bmatrix} \partial_x \varphi_0^{\text{IM}} \\ \partial_y \varphi_0^{\text{IM}} \end{bmatrix} = \begin{bmatrix} e_1 \\ e_2 \end{bmatrix}. \quad (6)$$

The coefficients have the form

$$\begin{aligned} a_{m,1} &= c_{m,4} I_0^{\text{CCD}} + c_{m,1} \frac{\lambda dz}{2\pi} \partial_x I_0^{\text{CCD}}, \\ a_{m,2} &= c_{m,5} I_0^{\text{CCD}} + c_{m,1} \frac{\lambda dz}{2\pi} \partial_y I_0^{\text{CCD}}, \\ e_m &= d_m - c_{1,1} I_0^{\text{CCD}} - c_{1,2} \partial_x I_0^{\text{CCD}} - c_{1,3} \partial_y I_0^{\text{CCD}}. \end{aligned} \quad (7)$$

After the phase derivatives  $\partial_x \varphi_0^{\text{IM}}$  and  $\partial_y \varphi_0^{\text{IM}}$  are solved from Eq. (4) or Eq. (6), the desired phase  $\varphi_0^{\text{IM}}$  can be obtained by using the Frankot–Chellappa algorithm [28]:

$$\varphi_0^{\text{IM}}(x, y) = \text{FT}^{-1} \left\{ \frac{\text{FT}\{\partial_x \varphi_0^{\text{IM}}\}}{ik_x} \right\} + \left\{ \frac{\text{FT}\{\partial_y \varphi_0^{\text{IM}}\}}{ik_y} \right\}. \quad (8)$$

In the traditional TIE method, the phase is retrieved from the second-order TIE phase derivatives, and knowledge of the boundaries is needed [22]. The proposed method reconstructs the phase from the first-order derivatives and avoids the difficulty of determining the boundary conditions. The traditional TIE produces artifacts when the object wavefront has low-frequency modulation, while the modulated illumination used here produces a high frequency and thus improves the SNR of the phase imaging [29]. However, just like the traditional TIE [18–25], this method can only be used for samples with continuous phase, since Eq. (8) relies on the hypothesis that the wavefront function  $\varphi_0^{\text{IM}}(x, y)$  is differentiable everywhere [28].

Based on the configuration shown in Fig. 1, an experiment has been carried out to demonstrate the feasibility of the method. The light source was a laser diode with wavelength 635 nm, and a SLM was used to generate the illuminations. The magnification of the imaging unit composed of the lenses  $L_3$  and  $L_4$  was 50X, and the numerical aperture  $\text{NA} = 0.25$ . The specimen was a slice of mouse kidney adjusted such that its image became slightly defocused on the CCD. The distance  $dz$  was 1 mm

and has been determined by loading a grating on the SLM and detecting the lateral shear. Five random patterns were loaded sequentially on the SLM to generate spatially modulated illuminations; their intensities are shown schematically in Fig. 2(a). The phases of these illuminations were measured by the interferometric [4] and referenceless phase retrieval methods [30], and it was found that the results agree with the phases simply calculated from the gray value of the patterns loaded on the SLM. The diffraction patterns of the sample under these illuminations are shown in Fig. 2(b). The recorded intensity obtained when a plane wave was used to illuminate the sample is shown in Fig. 2(c). By using Eq. (4), the phase derivatives of the sample in  $x$  and  $y$  directions are obtained; the derivative along the  $x$  direction is shown in Fig. 2(d). The phase distribution of the sample is reconstructed from the derivatives by using Eq. (7) and is shown in Fig. 2(e). For comparison, the same sample was also investigated by digital holographic microscopy (DHM), and the result is shown in Fig. 2(f). The consistency between the two figures verifies the feasibility of the proposed method.

When the phase has discontinuities, an iterative process can be applied where the object wave (we denote it as  $O_0 = \sqrt{I_0^{\text{IM}}} \exp(i\varphi_0^{\text{IM}})$ ) obtained by the deterministic method is used as the initial value. The iterative phase retrieval is performed as follows: (1) Multiply  $O_0$  by the  $m$ th illuminations  $A_m^{\text{illum,IM}}$  (with  $m = 1, 2, \dots, M$ ) and propagate to the CCD plane. (2) Replace the amplitude

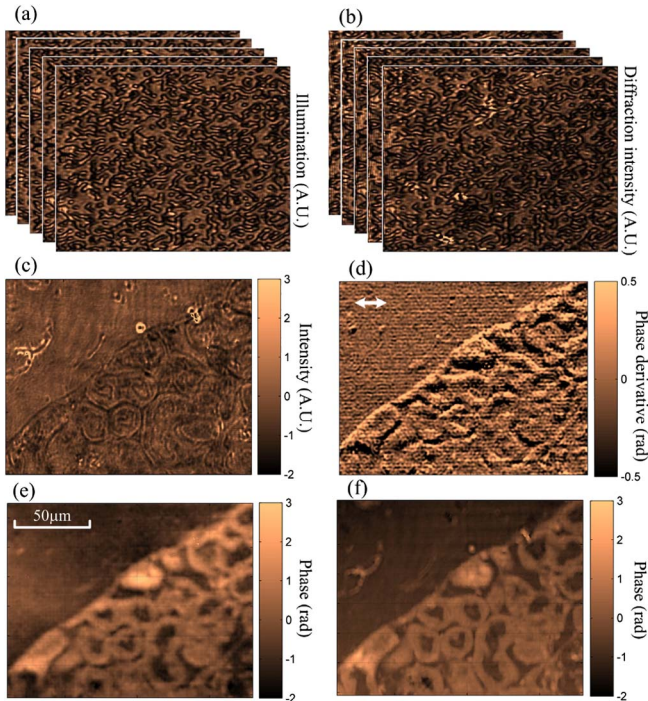


Fig. 2. Reconstruction results of a slice of mouse kidney. (a) Intensity distributions of five illuminations, (b) intensity distributions of five generated diffraction patterns, (c) intensity image of the sample under plane wave illumination, (d) reconstructed phase derivative of the object wave in the  $x$  direction, (e) the reconstructed phase distributions obtained by the proposed method, and (f) those obtained by DHM. The arrow in (d) denotes the direction of the phase derivative.

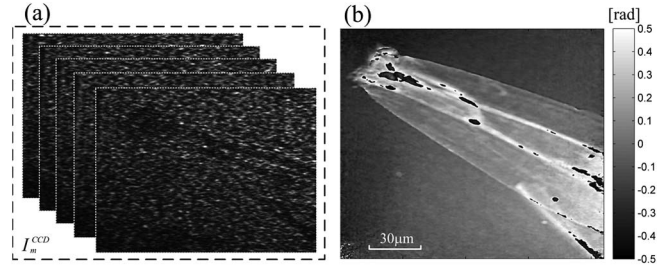


Fig. 3. Phase retrieval on the wing of a mosquito. (a) Diffraction patterns under five spatially modulated illuminations and (b) phase distribution of the wavefront transmitted by the wing of the mosquito.

of the obtained object wave with  $\sqrt{I_m^{\text{CCD}}}$ . (3) Propagate the obtained wave to the IM, and denote it as  $A_m^{\text{Obj}}$ . (4) Replace the initial object wave  $O_0$  with the improved object wave  $O_{\text{impr}} = A_m^{\text{Obj}} / A_m^{\text{illum,IM}}$ . (5) Repeat the iteration loop (2)–(4) by using  $m + 1$  instead of  $m$ , until the difference between two neighboring reconstructions is smaller than a threshold value. The coherent noise can be further suppressed by averaging the different object wave  $O_{\text{impr}}$  reconstructed from different groups of the modulated illuminations. For the deterministic phase retrieval method, the distance  $dz$  between the image and CCD planes is chosen to have a small value (typically  $M_0^2 \lambda / \text{NA}^2$ , where  $M_0$  and  $\text{NA}$  are the magnification and numerical aperture of the imaging system) in order to have a good approximation when we replace  $\partial I / \partial z$  with  $(I_m^{\text{CCD}} - I_m^{\text{IM}}) / dz$  in Eq. (8). For the iterative method, the above approximation is not required, and  $dz$  can be larger.

The sample used to demonstrate the feasibility of the iterative method was a mosquito wing, producing a wavefront with phase discontinuities. The defocus distance  $dz$  between the IM and the CCD plane was 10 mm. Twenty random spatially modulated waves were used to illuminate the sample, and the generated diffraction patterns were recorded; five of them are shown in Fig. 3(a). The

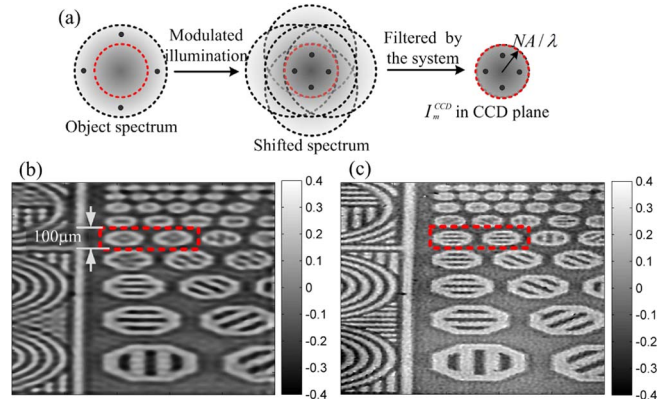


Fig. 4. Resolution enhancement. (a) Spectrum evolution of the object wave during the imaging process. The red dashed rings denote the frequency limited by the NA of the imaging system. The four black dots denote the frequency components, which are beyond the theoretical resolution limit. (b) Phase images reconstructed by DHM with plane wave illumination and (c) the phase retrieval with spatially modulated illumination.

recovered phase of the wavefront is shown in Fig. 3(b). The sharp phase image with the clear background shows the feasibility of the method.

The spatially modulated illuminations can also improve the spatial resolution of the phase imaging. Usually, the imaging resolution is limited by the aperture of the imaging system, which truncates the high-frequency components [denoted by the four dots in Fig. 4(a)]. As shown in Fig. 4(a), the spatially modulated illumination scrambles the specimen spectrum, and thus some high-frequency components of the object wave beyond the NA of the system are downshifted and pass through the system. These high-frequency components are shifted back to their original positions during the iterative process, and the resolution of the imaging is improved. A transparent structured plate was used as the specimen for the experimental demonstration. The magnification of the second telescope system (composed of the lenses  $L_3$  and  $L_4$ ) has a lower NA of 0.021, and thus the resolution of the setup is limited to  $\delta = 0.61\lambda/NA = 18 \mu\text{m}$  for the on-axis plane wave illumination. According to the resolution analysis [31], the spatially modulated illumination with the maximal diffraction angle of  $\theta_{\text{max}} = 0.018$  rad improves the resolution to  $\delta_{\text{improv}} = 0.61\lambda/(NA + \sin \theta_{\text{max}}) = 10 \mu\text{m}$ . The images reconstructed by using DHM with on-axis plane wave illumination and the phase retrieval method are shown in Figs. 4(b) and 4(c), respectively. The comparison between these two figures shows that the resolution was improved by the spatially modulated illumination. The structures with linewidth  $12.5 \mu\text{m}$  that are not resolvable in Fig. 4(b) are resolved in Fig. 4(c). Low-NA lenses were used in our setup for phase imaging of a very large specimen, but high-NA objectives can be used as well.

To sum up, a phase retrieval method based on spatially modulated illuminations is proposed. Deterministic phase retrieval is performed for the sample with smooth phase distribution without the iteration process, and the boundary problem in the traditional TIE method is avoided. An iterative method, which starts with the object wave obtained by using the deterministic phase retrieval method, is used to reconstruct continuous and discontinuous phase distributions with increased resolution. The TIE-based deterministic phase retrieval method has higher contrast on the edges of the sample, since the high-frequency spectrum is enhanced by the Laplacian operator. This artifact can be removed by using the iterative method. Due to the modulated illumination, this method has a small depth of focus and is thus only suitable for a sample with a thickness less than  $\lambda/(NA_{\text{illum}})^2$ , where  $NA_{\text{illum}}$  is the numerical aperture of the illumination. It should be considered as well that  $NA_{\text{illum}}$  should be always smaller than the NAs of the imaging system within this method.

P. Gao gratefully acknowledges the support of the Alexander von Humboldt Foundation. This research is

also supported by the German Science Foundation (DFG OS111/36-1) and National Natural Science Foundation of China (NSFC, 61107003 and 61377008).

## References

1. G. Popescu, T. Ikeda, K. Goda, C. A. Best-Popescu, and M. Laposata, *Phys. Rev. Lett.* **97**, 218101 (2006).
2. S. A. Alexandrov, T. R. Hillman, T. Gutzler, and D. D. Sampson, *Phys. Rev. Lett.* **97**, 168102 (2006).
3. B. Kemper and G. von Bally, *Appl. Opt.* **47**, A52 (2008).
4. C. Kohler, X. Schwab, and W. Osten, *Appl. Opt.* **45**, 960 (2006).
5. B. C. Platt and R. Shack, *J. Refract. Surg.* **17**, S573 (2001).
6. J. B. Costa, *Appl. Opt.* **44**, 60 (2005).
7. S. Dong, T. Haist, and W. Osten, *Appl. Opt.* **51**, 6268 (2012).
8. P. Bon, G. Maucort, B. Wattellier, and S. Monneret, *Opt. Express* **17**, 13080 (2009).
9. G. Pedrini, W. Osten, and Y. Zhang, *Opt. Lett.* **30**, 833 (2005).
10. P. Almero, G. Pedrini, and W. Osten, *Appl. Opt.* **45**, 8596 (2006).
11. P. Bao, F. Zhang, G. Pedrini, and W. Osten, *Opt. Lett.* **33**, 309 (2008).
12. Y. J. Liu, B. Chen, E. R. Li, J. Y. Wang, A. Marcelli, S. W. Wilkins, H. Ming, Y. C. Tian, K. A. Nugent, P. P. Zhu, and Z. Y. Wu, *Phys. Rev. A* **78**, 023817 (2008).
13. F. Zhang, G. Pedrini, and W. Osten, *Phys. Rev. A* **75**, 043805 (2007).
14. F. Zhang and J. M. Rodenburg, *Phys. Rev. B* **82**, 121104(R) (2010).
15. J. M. Rodenburg and H. M. L. Faulkner, *Appl. Phys. Lett.* **85**, 4795 (2004).
16. H. M. L. Faulkner and J. M. Rodenburg, *Phys. Rev. Lett.* **93**, 023903 (2004).
17. T. B. Edo, D. J. Batey, A. M. Maiden, C. Rau, U. Wagner, Z. D. Pešić, T. A. Waigh, and J. M. Rodenburg, *Phys. Rev. A* **87**, 053850 (2013).
18. M. R. Teague, *J. Opt. Soc. Am.* **72**, 1199 (1982).
19. M. R. Teague, *J. Opt. Soc. Am. A* **2**, 2019 (1985).
20. F. Roddier, *Appl. Opt.* **29**, 1402 (1990).
21. J. Frank, S. Altmeyer, and G. Wernicke, *J. Opt. Soc. Am. A* **27**, 2244 (2010).
22. C. Zuo, Q. Chen, Y. Yu, and A. Asundi, *Opt. Express* **21**, 5346 (2013).
23. A. V. Martin, F. R. Chen, W. K. Hsieh, J. J. Kai, S. D. Findlay, and L. J. Allen, *Ultramicroscopy* **106**, 914 (2006).
24. L. J. Allen and M. P. Oxley, *Opt. Commun.* **199**, 65 (2001).
25. P. Bon, S. Monneret, and B. Wattellier, *Appl. Opt.* **51**, 5698 (2012).
26. J. Stoer and R. Bulirsch, *Introduction to Numerical Analysis* (Springer, 1980).
27. W. Osten, *Proc. SPIE* **0473**, 52 (1985).
28. R. T. Frankot and Z. Chellappa, *IEEE Trans. Pattern Anal. Mach. Intell.* **10**, 439 (1988).
29. P. F. Almero, L. Waller, M. Agour, C. Falldorf, G. Pedrini, W. Osten, and S. G. Hanson, *Opt. Lett.* **37**, 2088 (2012).
30. P. Gao, G. Pedrini, and W. Osten, *Opt. Lett.* **38**, 5204 (2013).
31. W. Osten and N. Reingand, eds., *Optical Imaging and Metrology: Advanced Technologies* (Wiley-VCH, 2012).